J|A|C|S
ARTICLES

Published on Web 12/02/2009

Electrostatically Self-Assembled Polyoxometalates on Molecular-Dye-Functionalized Diamond

Yu Lin Zhong, Wibowo Ng, Jia-Xiang Yang, and Kian Ping Loh*

Department of Chemistry, National University of Singapore, 3 Science Drive 3, Singapore 117543

Received May 22, 2009; E-mail: chmlohkp@nus.edu.sg

Abstract: We have successfully immobilized phosphotungstic acid (PTA), a polyoxometalate, on the surface of boron-doped diamond (BDD) surface through electrostatic self-assembly of PTA on pyridinium dye-functionalized-BDD. The inorganic/organic bilayer structure on BDD is found to exhibit fast surface-confined reversible electron transfer. The molecular dye-grafted BDD can undergo controllable electrical stripping and regeneration of PTA which can be useful for electronics or sensing applications. Furthermore, we have demonstrated the use of PTA as a molecular switch in which the direction of photocurrent from diamond to methyl viologen is reversed by the surface bound PTA. Robust photocurrent converter based on such molecular system-diamond platform can operate in corrosive medium which is not tolerated by indium tin oxide electrodes.

I. Introduction

Diamond is an extraordinary material with outstanding properties such as optical transparency, chemical robustness, wide electrochemical potential window, and biocompatibility. The chemical vapor deposition (CVD) of boron-doped nanocrystalline diamond (NCD) on glass and quartz[1] opens up possibilities of using diamond as an alternative electrode for photovoltaics compared to optically transparent electrodes (OTEs).[2] The surface of diamond can be considered as a solid organic template, and chemically robust C−C bonds can be formed via covalent coupling. To derivatize diamond with functional molecules, photochemical coupling with alkenes[3] as well as electrochemical modification via reduction of aryldiazonium salts had been applied successfully. Aryldiazonium salts have been applied to functionalize various metals and semiconductors[4] in many fields ranging from combinatorial chemistry to molecular electronics.[5] Variations of the diazonium coupling chemistry include spontaneous grafting via charge exchange[6] or the electrochemical grafting of in situ generated aryldiazonium salts.[7]

The functionalization of diamond by electrochemical reduction of aryldiazonium salts was first reported by Kuo et al.[8] and much interest was generated subsequently,[9] especially in connection with the biofunctionalization of diamond.[10] Precise control of grafted organics density via electrochemical reduction of aryldiazonium salts is not a straightforward task. A comprehensive review by Pinson and Podvorica[11] discussed monolayer grafting achieved by the careful control of grafting parameters such as the amount of charge supplied during electrochemical grafting and the concentration of aryldiazonium salts. A Monte Carlo simulation of attaching 4-bromobenzene on Si(111) performed by Allongue et al.[12] indicated that the formation of organized domains is related to the higher probability of grafting a molecule in the neighborhood of a first attached molecule, arising from $\pi-\pi$ stacking interactions between neighboring adsorbates. The importance of stacking interactions was also

(1) Williams, O.; Nesladek, M. In *Physics and Applications of CVD Diamond*; Koisumi, S., Nebel, C. E., Nesladek, M., Eds.; Wiley-VCH: New York, 2008; p 13.
(2) Zhong, Y. L.; Midya, A.; Ng, Z.; Chen, Z.-K.; Daenen, M.; Nesladek, M.; Loh, K. P. *J. Am. Chem. Soc.* **2008**, *130*, 17218.
(3) (a) Yang, W.; Auciello, O.; Bulter, J. E.; Cai, W.; Carlisle, J. A.; Gerbi, J. E.; Gruden, D. M.; Knickerbocker, T.; Lasseter, T. L.; Russell, J. N., Jr.; Smith, L. M.; Hamers, R. J. *Nat. Mater.* **2002**, *1*, 253. (b) Hartl, A.; Schmich, E.; Garrido, J. A.; Hernado, J.; Catharion, S. C. R.; Walter, S.; Feulner, P.; Kromka, A.; Steinmuller, D.; Stutzmann, M. *Nat. Mater.* **2004**, *3*, 736. (c) Zhong, Y. L.; Chong, K. F.; May, P. W.; Chen, Z.-K.; Loh, K. P. *Langmuir* **2007**, *23*, 5824. (d) Chong, K. F.; Loh, K. P.; Vedula, S. R. K.; Lim, C. T.; Sternschulte, H.; Steinmüller, D.; Sheu, F.-S.; Zhong, Y. L. *Langmuir* **2007**, *23*, 5615.
(4) (a) Jiang, D.; Sumpter, B. G.; Dai, S. *J. Am. Chem. Soc.* **2006**, *128*, 6030. (b) Stewart, M. P.; Maya, F.; Kosynkin, D. V.; Dirk, S. M.; Stapleton, J. J.; McGuiness, C. L.; Allara, D. L.; Tour, J. M. *J. Am. Chem. Soc.* **2004**, *126*, 370. (c) Corgier, B. P.; Marquette, C. A; Blum, L. J *J. Am. Chem. Soc.* **2005**, *127*, 18328. (d) Marwan, J.; Addou, T.; Bélanger, D. *Chem. Mater.* **2005**, *17*, 2395. (e) Price, B. K.; Hudson, J. L.; Tour, J. M. *J. Am. Chem. Soc.* **2005**, *127*, 14867.
(5) (a) Coulon, E.; Pinson, J.; Bourzat, J.-D.; Commerçon, A.; Pulicani, J.-P. *J. Org. Chem.* **2002**, *67*, 8513. (b) Kosynkin, D. M.; Tour, J. M. *Org. Lett.* **2001**, *3*, 993.
(6) Adenier, A.; Cabet-Deliry, E.; Chaussé, A.; Griveau, S.; Mercier, F.; Pinson, J.; Vautrin-Ul, C. *Chem. Mater.* **2005**, *17*, 491–501.
(7) Baranton, S.; Bélanger, D. *J. Phys. Chem. B* **2005**, *109*, 24401.
(8) Kuo, T. C.; McCreery, R. L.; Swain, G. M. *Electrochem. Solid-State Lett.* **1999**, *2*, 288.
(9) (a) Wang, J.; Firestone, M. A.; Auciello, O.; Carlisle, J. A. *Langmuir* **2004**, *20*, 11450. (b) Shin, D.; Rezek, B.; Tokuda, N.; Takeuchi, D.; Watanabe, H.; Nakamura, T.; Yamamoto, T.; Nebel, C. E. *Phys. Status Solidi A* **2006**, *203*, 3245. (c) Uetsuka, H.; Shin, D.; Tokuda, N.; Saeki, K.; Nebel, C. E. *Langmuir* **2007**, *23*, 3466.
(10) (a) Wang, J.; Carlisle, J. A. *Diamond Relat. Mater.* **2006**, *15*, 279. (b) Zhou, Y. L.; Zhi, J. F. *Electrochem. Commun.* **2006**, *8*, 1811. (c) Shin, D.; Tokuda, N.; Rezek, B.; Nebel, C. E. *Electrochem. Commun.* **2006**, *8*, 844.
(11) Pinson, J.; Podvorica, F. *Chem. Soc. Rev.* **2005**, *34*, 429.
(12) Allongue, P.; Henry de Villeneuve, C.; Cherouvrier, G.; Cortès, R.; Bernard, M. -C. *J. Electroanal. Chem.* **2003**, *550−551*, 161.

demonstrated by Lud et al.[13] in the formation of biphenyl self-assembled monolayers on doped ultrananocrystalline diamond via spontaneous grafting without electrochemical induction. In addition, the chemical reduction potential of the different aryldiazonium salts with respect to the Fermi level of the solid surface controls the extent of reaction.[14] Thus far, most of the diazonium salts grafted are restricted to nitrophenyl or bromophenyl moieties due to the ease of acquiring these commercially. In principle the concept of diazonium grafting can be extended to a wide range of molecules, including organic dyes or charged molecules, although this has not been explored on the diamond platform.

Due to the rich and versatile electrochemical and photochemical properties of polyoxometalates (POM), they have attracted great attention in field of analytical chemistry, catalysis, biology, medicine, and materials science.[15] Of particular interest is the bottom up fabrication of POM-based materials with atomic precision through growth processes determined by self-assembly for constructing modular molecular nanosystems. Some of the popular methods include the use of Langmuir−Blodgett (LB) technique[16] and electrostatic layer-by-layer self-assembly (ELSA) method[17] to provide control of film thickness, structure, and function. To create a more robust device, schemes based on the covalent attachments of POMs through organic linkers had been developed.[18] Herein we report a strategy to graft a dye molecule onto diamond via the facile electrochemical reduction of in situ generated aryldiazonium salt, which allows subsequent electrostatic assembly of phosphotungstic acid (PTA), a type of POM, onto the positively charged terminal pyridinium end of the coupled dye. The electrostatic interactions among the charged groups can help to stabilize film structure and prevent molecular aggregation, leading to the formation of well-ordered molecular clusters.

II. Experimental Section

Chemical Reagents. All chemicals purchased were of the purest grade and used as received from Sigma-Aldrich unless otherwise stated. Phosphotungstic acid hydrate ($H_3[P(W_3O_{10})_4]\cdot xH_2O$), also known as tungstophosphoric acid, was used as received. All solvents used for reaction and rinsing were of HPLC grade unless otherwise stated. All dilution and preparation of electrolytes for electrochemical work were made with Nanopure water (18.0 MΩ·cm).

Organic Synthesis. 1-Butyl-4-methylpyridinium Bromide (1). 1-Bromobutane (10 mL, 0.102 mol) was added to freshly distilled 4-picoline (12.1 mL, 0.112 mol) under nitrogen; 95% ethanol (125 mL) was added, and the mixture was refluxed for 24 h (see Scheme 1). Light brownish-yellow crystals were precipitated upon cooling in the refrigerator. The product was filtered and washed with ethyl acetate and subsequently dried under vacuum with a yield of 50%.[19]

Scheme 1. Synthesis of 1-butyl-4-methylpyridinium Bromide

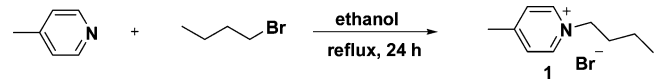

4-Aminobenzaldehyde (2). Grounded sulfur flakes (5 g), sodium sulfide nanohydrate (10 g, 41.7 mmol), and sodium hydroxide (9 g, 0.223 mol) were added to 200 mL of deionized water and then heated for 20 min on a steam bath. Next, the mixture was added to a hot solution of 4-nitrotoluene (16.7 g, 0.103 mol) in 95% ethanol (100 mL), and the resulting mixture was refluxed at 80 °C for 3 h. Deionized water (300 mL) was added to this mixture which was then subjected to rapid vacuum distillation. The distillation was terminated when the volume of residue decreased to about 200 mL. Following that, the residual flask was immersed in an ice bath for 2 h for crystallization. Yellow-orange crystals of the product were obtained via vacuum filtration and then purified by washing with (200 mL) of cold, deionized water. The product was dried over potassium hydroxide pellets in a vacuum desiccator for 24 h, giving a yield of approximately 45%.[20]

4-(4-Aminostyryl)-1-butylpyridinium Bromide (3). 1-Butyl-4-methylpyridinium bromide (4 g, 29.2 mmol) and 4-aminobenzaldehyde (2.36 g, 19.5 mmol) were added to 95% ethanol (60 mL) and refluxed at 80 °C for 24 h (see Scheme 2). The mixture was then allowed to cool gradually before placing it in an ice bath for crystallization to occur. Reddish-purple crystals were obtained by vacuum filtration with a yield of 75%. ^{1}H NMR (DMSO, 300 MHz) δ: 0.90 (3H, t, $J = 7.50$ Hz), 1.26 (2H, m), 1.86 (2H, m), 4.40 (2H, t, $J = 7.20$ Hz), 6.01 (2H, s), 6.62 (2H, d, $J = 8.70$ Hz), 7.09 (1H, d, $J = 15.90$ Hz), 7.46 (2H, d, $J = 8.70$ Hz), 7.86 (1H, d, $J = 16.2$ Hz), 8.03 (2H, d, $J = 6.90$ Hz), 8.75 (2H, d, $J = 6.90$ Hz). ^{13}C NMR (DMSO, 300 MHz): 13.30, 18.75, 32.41, 58.81, 113.74, 116.33, 122.23, 122.41, 130.53, 142.57, 143.39, 152.10, 153.84. ESI-MS: *m/z* 254.2, 197.3. FT-IR (KBr, cm^{-1}): 3349, 3285, 3181, 3032, 2962, 2917, 1619, 1585, 1470, 1375, 1313, and 1165.

Diamond Thin Film. Polycrystalline boron-doped diamond (BDD) films (50 μm thick) were grown on *p*-type Si substrates in a commercial 2.45 GHz microwave plasma reactor (Astex) using methanol and boron oxide mixtures. The BDD samples had a surface resistance of 10 Ω cm and the boron doping level was approximately 10^{20} cm^{-3}. These BDD samples were used for electrochemical experiments due to their high conductivity. Optically transparent diamond electrode was fabricated by the CVD of a thin layer of boron-doped diamond film on quartz substrate (160 nm thick, boron concentration 7×10^{20} cm^{-3}) according to published procedures.[1]

Acid cleaning and hydrogen plasma cleaning of diamond were used for all diamond samples. Metallic impurities were first dissolved in hot aqua regia (HNO_3/HCl = 1:3), followed by the removal of organic impurities from the diamond samples by hot "piranha" solution (H_2O_2/H_2SO_4 = 1:3) at 90 °C for 1 h. Hydrogen termination of diamond samples was attained by microwave hydrogen plasma treatment using 800 W microwave power and 300 sccm of hydrogen gas flow for 15 min.

Surface Reaction Conditions. The grafting of the molecular dye on H-terminated BDD via electrochemical reduction of in situ generated aryldiazonium salt was carried out by applying five cyclic voltammetric scans between +0.5 and −0.8 V (vs Ag/AgCl) with a scan rate of 100 mV/s, in a solution of 1 mM of the tailor-made molecular dye (**3**) and 1 mM $NaNO_2$ in 0.5 M HBF_4. The grafted substrate was then ultrasonicated in acetone to remove any physisorbed molecules, followed by rinsing in ethanol and water.

(13) Lud, S. Q.; Steenackers, M.; Jordan, R.; Bruno, P.; Gruen, D. M.; Feulner, P.; Garrido, J. A.; Stutzmann, M. *J. Am. Chem. Soc.* **2006**, *128*, 16884.
(14) Zhong, Y. L.; Loh, K. P.; Midya, A.; Chen, Z.-K. *Chem. Mater.* **2008**, *20*, 3137.
(15) (a) Hill, C. L. *Chem. Rev.* **1998**, *1*, 98 (Thematic Issue). (b) Pope, M. T.; Müller, A. *Polyoxometalate Chemistry: From Topology via Self-Assembly to Applications*; Kluwer: Dordrecht, The Netherlands, 2001.
(16) Liu, L.; Ai, W.-H.; Li, M.-J.; Liu, S.-Z.; Zhang, C.-M.; Yan, H.-X.; Du, Z.-L.; Wong, W.-Y. *Chem. Mater.* **2007**, *19*, 1704.
(17) Liu, S.; Kurth, D. G.; Bredenkötter, B.; Volkmer, D. *J. Am. Chem. Soc.* **2002**, *124*, 12279.
(18) (a) Mayer, C. R.; Nevus, S.; Cabuil, V. *Angew. Chem., Int. Ed.* **2002**, *41*, 501. (b) Errington, R. J.; Petkar, S. S.; Horrocks, B. R.; Houlton, A.; Lie, L. H.; Patole, S. N. *Angew. Chem., Int. Ed.* **2005**, *44*, 1254. (c) Lu, M.; Nolte, W. M.; He, T.; Corley, D. A.; Tour, J. M. *Chem. Mater.* **2009**, *21*, 442.
(19) Behar, D.; Neta, P.; Schultheisz, C. *J. Phys. Chem. A* **2002**, *106*, 3139.
(20) (a) Campaigne, E.; Budde, W. M.; Schaefer, G. F. *Org. Synth.* **1963**, *4*, 31. (b) Ogata, Y.; Kawasaki, A.; Sawaki, Y.; Nakagawa, Y. *Bull. Chem. Soc. Jpn.* **1979**, *52*, 2399.

Electrostatic self-assembly of phosphotungstic acid (PTA) was performed by immersing the molecular-dye-functionalized BDD (BDD + dye) in 10 mM PTA for 1 min. After all coupling steps, the substrates were rinsed copiously with acetone, ethanol, and ultrapure water to remove any physisorbed molecules.

Instrumentations. X-ray photoelectron spectroscopy (XPS) was performed with a Phobios 100 electron analyzer (SPECS GmbH) equipped with 5 channeltrons, using an unmonochromated Al Kα X-ray source (1486.6 eV). The pass energy of the hemisphere analyzer was set at 50 eV for wide scan and 20 eV for narrow scan, while the takeoff angle was fixed at normal to the sample. Ultraviolet photoelectron spectroscopy (UPS) was performed using He I UV lamp (VG Microtech, UK) with the same electron analyzer at pass energy of 1 eV. The sample was biased at −5 V to overcome the analyzer function of 4.44 eV in order to observe a distinct low energy cutoff.

The thickness of grafted molecular film was characterized by atomic force microscopy (AFM) scratching experiments performed using the NanoMan AFM system (Veeco Instruments and Process Metrology, USA) operating under contact mode for scratching and tapping mode for imaging. A large force of >120 nN was employed to scratch an area of 1 μm^2 with complete removal of organic, and thereafter an area of 5 μm^2 was directly imaged under the tapping mode. BudgetSensor Multi75 cantilever (Innovative Solutions Bulgaria Ltd., Bulgaria) with a typical resonant frequency of 75 kHz and a force constant of 3 N/m was employed throughout this study. Loading forces during the scratching experiments were calculated from force curve measurements for each cantilever.

All electrochemical measurements were carried out with an Autolab PGSTAT30 potentiostat (Eco Chemie, The Netherlands). Photoelectrochemical measurements were performed in 0.1 M Na_2SO_4 solution containing 5 mM methyl viologen (MV^{2+}) as an electron carrier, in a custom-made photoelectrochemical Teflon cell with three-electrode configuration system: a diamond working electrode, Ag/AgCl reference electrode (3.0 M KCl), and a Pt mesh counter-electrode.[2] Top contact on the sample surface (spotted with Ag paste for improved contacts) was made through Au-plated strips. The area of the sample exposed to light was 0.196 cm^2.

Action spectrum was obtained by a monochromatic irradiation produced by a Newport 300 W xenon light source, through a Newport Cornerstone 260 monochromator. The light intensity was measured by a Newport calibrated Si detector to be 0.35 mW/cm^2 at 440 nm. The currents were measured in light intensity under steady state.

Solid-state UV−visible spectra were acquired using UV−visible spectrophotometry (Shimadzu UV-2450). A 1 cm × 1 cm H-terminated boron-doped nanocrystalline diamond grown on quartz plate was used to calibrate the instrument before characterization and employed as a reference throughout the experiment. Another identical substrate was grafted with dye and later immersed in the PTA solution for the electrostatic self-assembly.

The absorption spectrum and structural configuration of the dye was simulated using both density functional theory (DFT) and semiempirical methods. A comparison between DFT and the semiempirical method regarding the geometry of the molecular dye was made. DFT calculation was performed using the DMol3 code.[21] The exchange and correlation energies were calculated with the PWC functional of the local density approximation (LDA).[22] Semiempirical quantum mechanical calculation was performed using the VAMP (Vienna *ab initio* Molecular-Dynamics Package)[23] modules with the Austin model Hamiltonian of first degree (AM1).[24] The AM1 was chosen because it contains parameters for elements that this molecular dye contains (H, C, N, F, and B).[25] The semiempirical calculation gives similar results as DFT calculations; the degree of error is less than 4%. After geometry optimization, the UV−visible spectrum of the dye was simulated by calculating the electronic transition using VAMP.

Scheme 2. Synthesis of 4-(4-Aminostyryl)-1-butylpyridinium Bromide

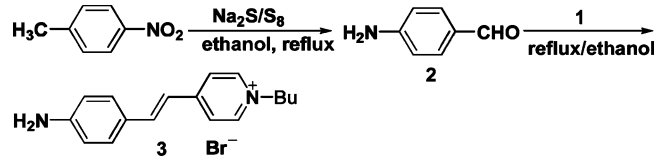

Scheme 3. Electrochemical Grafting of Molecular Pyridinium Dye Followed by Electrostatic Self-Assembly of PTA

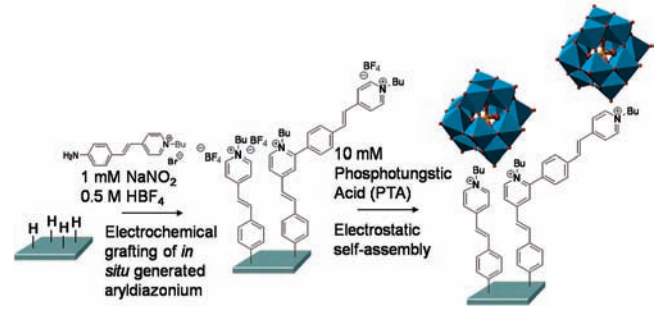

III. Results and Discussion

Diazonium Functionalization and Electrostatic Self-Assembly of PTA. The hierarchical assembly begins with the use of a tailor-made highly π-conjugated chromophore (**3**) which consists of a terminal pyridinium moiety, electron-rich phenylethyl core, and a reactive aniline group for diazotization, as shown in Scheme 3. The presence of pyridinium ion helps to solubilize the otherwise insoluble molecular wire in aqueous acidic solution, where $NaNO_2$ was added to diazotize the aniline group. The grafting of the molecular dye on hydrogen-terminated boron-doped diamond initiates with the electrochemical reduction of in situ generated aryldiazonium salt on the surface. Owing to the nature of free radical grafting and excessive reduction voltage (5 cycles to −0.8 V, vs Ag/AgCl), the possibility of multilayer formation cannot be excluded. The sample was subsequently rinsed and immersed in phosphotungstic acid (PTA) solution for electrostatic self-assembly. The advantages of electrochemical grafting via in situ generated aryldiazonium salts include the simplicity of storage, ease of working with stable aniline precursors, and compatibility with lithographical patterning. In Figure 1, the electrochemical grafting of in situ generated aryldiazonium salt can be judged from the board reduction peak (at 0 V vs Ag/AgCl) observed only in the first CV scan. The absence of reduction peak in subsequent scans indicates that the diamond electrode was fully passivated by bulky molecular dye after one scan.

Surface Science Characterization. The successful grafting of molecular dye was confirmed by X-ray photoelectron spectroscopy (XPS) as evident by the XPS N 1s peak at 402.1 eV

(21) (a) Delley, B. *J. Chem. Phys.* **1990**, *92*, 508. (b) Delley, B. *J. Chem. Phys.* **2000**, *113*, 7756.
(22) Perdew, J. P.; Wang, Y. *Phys. Rev. B* **1992**, *45*, 13244.
(23) Clark, T.; Alex, A.; Beck, B.; Burkhardt, F.; Chandrasekhar, J.; Gedeck, P.; Horn, A. H. C.; Hutter, M.; Martin, B.; Rauhut, G.; Sauer, W.; Schindler, T.; Steinke, T. *Vamp 8.1*; University of Erlangen: Erlangen, Germany, 2002.
(24) Dewar, M. J. S.; Zoebisch, E. G.; Healy, E. F.; Stewart, J. J. *J. Am. Chem. Soc.* **1985**, *107*, 3902.
(25) (a) Dewar, M. J. S.; Jie, C.; Zoebisch, E. G. *Organometallics* **1988**, *7*, 513. (b) Dewar, M. J. S.; Zoebisch, E. G. *J. Mol. Struct.: Theochem* **1988**, *180*, 1.

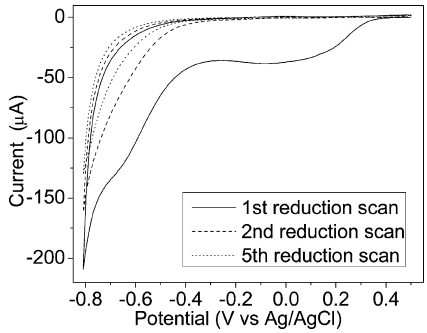

Figure 1. Cyclic voltammetry (CV) scans of H-terminated BDD in 1 mM molecular dye with equivalent $NaNO_2$ in 0.5 M HBF_4, from +0.5 to −0.8 V (vs Ag/AgCl) at 0.1 V/s.

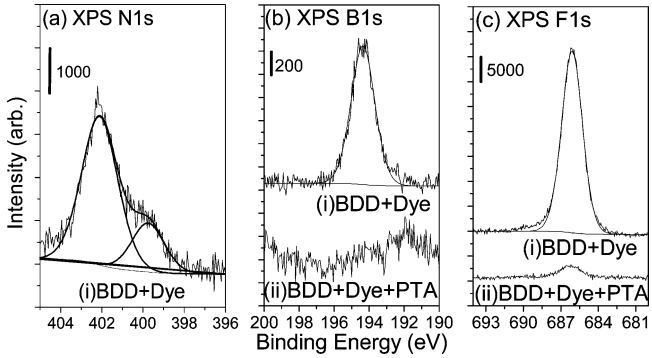

Figure 2. X-ray photoelectron spectroscopy (XPS) (a) N 1s spectrum of molecular-dye-functionalized BDD (BDD + dye). (b) B 1s and (c) F 1s spectrum of (i) molecular-dye-functionalized-BDD (BDD + dye) and (ii) electrostatically self-assembled PTA on dye-functionalized BDD (BDD + dye + PTA).

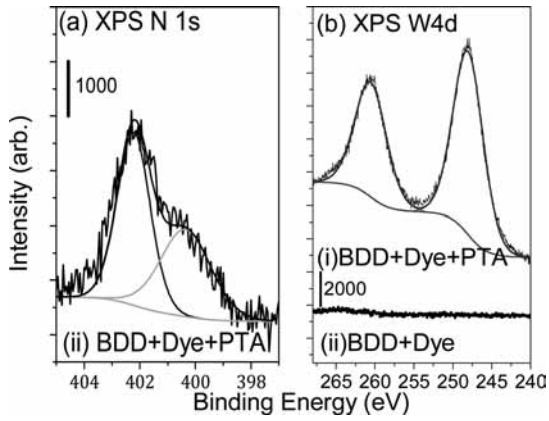

Figure 3. X-ray photoelectron spectroscopy (XPS) (a) N 1s of electrostatically self-assembles PTA on dye-functionalized BDD (BDD + dye + PTA) and (b) W4d spectra of (i) molecular-dye-functionalized-BDD (BDD + dye) and (ii) BDD + dye + PTA.

attributed to the pyridinium nitrogen (Figure 2a). The small peak at 399.8 eV is attributed to the formation of azo bridge in the molecular film which is characteristic of such an electrochemical grafting method.[26] From Table 1, the XPS elemental composition, after correction for relative atomic sensitivity factors, shows that original bromide counterions of the molecular dye were replaced by BF_4^- anion from HBF_4 and every surface pyridinium cation (at 402.1 eV) was matched with a BF_4^- counterion.

(26) Lyskawa, J.; Bélanger, D. *Chem. Mater.* **2006**, *18*, 4755.

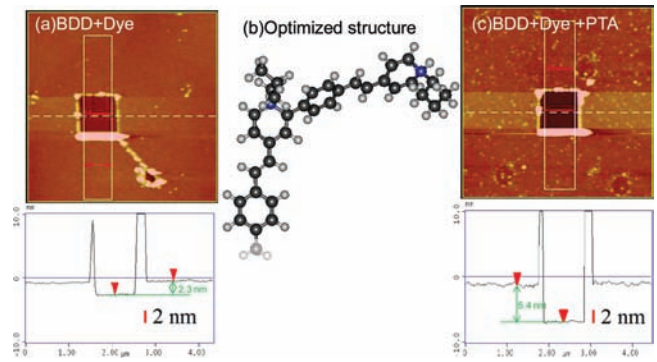

Figure 4. Tapping mode AFM image of scratched area on (a) molecular-dye-functionalized BDD (BDD + dye) and (c) electrostatically self-assembled PTA on dye-functionalized BDD (BDD + dye + PTA). (Bottom) Average line profiles through the scratched area showing an average height difference of 2.3 (±0.3) nm for (a) BDD + dye and 5.4 (±0.5) nm for (c) BDD + dye + PTA. (Center) (b) Computed heights of molecular dye and bilayer are 1.6 and 2.0 nm, respectively. The optimized structure shown has an additional methyl group (faded) to simulate the C−C bonding of the dye to the diamond surface.

Table 1. Elemental Composition of BDD + Dye

	integral (RSF corrected)	ratio
N 1s (402.1 eV)	4280	1
B 1s	4270	1
F 1s	17500	4.1

Table 2. Elemental Composition of BDD + Dye + PTA

	integral (RSF corrected)	ratio	expected ratio
N 1s (402.1 eV)	2650	1	1
W $4d_{5/2}$ (260.7 eV)	9220	3.5	4

Following ion exchange with PTAs, the BF_4 anions were replaced by the PTA. This is evidenced by the emergence of the XPS W 4d peaks as shown in Figure 3b and the diminished XPS B 1s and F 1s signals (Figure 2 and Table 1). Such an ion exchange method is a very versatile method to build up organic−inorganic hybrid films. From Table 2, the elemental ratio of N:W was calculated to be 1:3.5, which is close to the expected ratio of 1:4 to maintain electrical neutrality assuming one $PW_{12}O_{40}^{3-}$ is electrostatically bonded to three pyridinium groups. This suggests that most of the surface pyridinium groups were accessible to electrostatic binding with PTAs.

The thickness of the grafted molecular dye as well as the subsequently assembled PTA on diamond was verified by atomic force microscopy (AFM) scratching experiment. AFM was performed on a boron-doped single crystal diamond, C(100), with root-mean-square roughness of 0.165 nm. The corrugation of the clean surface is smaller than 10% of the step height fluctuations after the electrochemical grafting of the molecular dye and PTA adlayers on the surface. In AFM contact mode, a large force of more than 120 nN was employed to scratch an area of 1 μm^2 with complete removal of organic dye, and thereafter an area of 5 μm^2 was directly imaged under the tapping mode. Multiple domains were randomly chosen for imaging to get statistical sampling. From Figure 4, an average height profile was drawn through the scratched trench perpendicular to the scanning direction of the tip to minimize error arising from artifacts along the scanning direction. Multiple height measurements were taken within the sampling box (~4.4 $\mu m \times 0.8$ μm) drawn on the AFM image. The average molecular

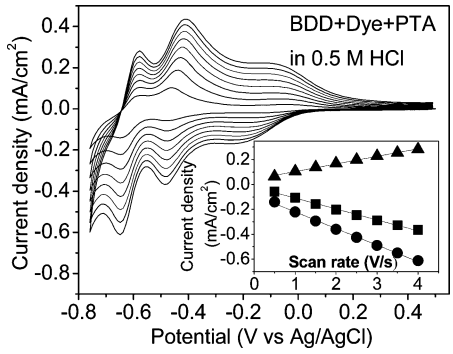

Figure 5. Cyclic voltammetry (CV) scans of electrostatically self-assembled PTA on dye-functionalized BDD (BDD + dye + PTA) in 0.5 M HCl at varying scan rate from 0.5 to 4 V/s. Inset shows plot of cathodic peak current at −0.48 V(■) and −0.65 V(●) and anodic peak current at −0.58 V(▲) vs scan rate.

dye thickness was found to be 2.3 ± 0.3 nm. This indicates that the organic film consisted of predominantly two monolayers. The definition of two monolayers is based on the theoretically optimized length of a first layer molecular dye covalently coupled to a second branched layer as shown in Figure 4b, where the energetically optimized structure is determined to have a projected vertical height of 2 nm. After electrostatic self-assembly of PTA, the increased average film thickness of 5.4 ± 0.5 nm confirmed the presence of PTA as shown in Figure 4c.

Electrochemical Characterization. Figure 5 shows the CV scans of electrostatically self-assembled PTA on dye-functionalized BDD (BDD + dye + PTA) in 0.5 M HCl, collected at different scan rates. It should be pointed out that experiments in harsh acidic conditions are impossible to perform with indium tin oxide (ITO) because of its chemical instability in acid. The advantage of using diamond is its chemical robustness.[27] The cathodic peak currents (at −0.48 and −0.65 V) and anodic peak current (at −0.58 V) show linear dependence on scan rate, which is indicative of a surface confined redox process (Figure 5, inset). The peak potentials remain constant up to the fastest scan rate of 400 mV/s, which indicate fast electron transfer between the BDD and PTA.

Using the Randles−Sevcik equation for a Nernstian reaction at the adsorbate monolayer (eq 1),[28]

$$i_p = (9.39 \times 10^5) n^2 \nu A \Gamma \qquad (1)$$

where i_p is the peak current in A, n is number of electrons, ν is the scan rate in V/s, A is the electrode surface area in cm^2, and Γ is the coverage in mol/cm^2. The plot of peak current at −0.48 V versus scan rate yields a straight line of equation: y = (9.54 × 10^{-5})x, which fits the data with an R^2 value of 0.998. With n = 1 and A = 0.283 cm^2, Γ was calculated to be 2.2 × 10^{14} molecules/cm^2, which corresponds to about two monolayers of PTA.[29] This result correlates well with our AFM studies and proves the formation of bilayered molecular film in which all the pyridinium ions are accessible to PTA. It is known that the surface coverage is directly related to the total charge of the PTA anion and can be controlled from submonolayer to multilayer coverage by adjusting the ionic strength of the dipping solutions. Interestingly, the electrostatically self-assembled PTA

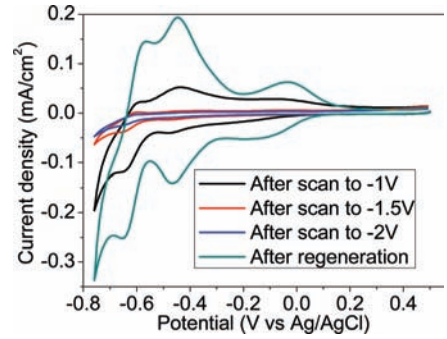

Figure 6. CV scans of electrostatically self-assembled PTA on molecular-dye-functionalized BDD (BDD + dye + PTA) in 0.5 M HCl at scan rate of 1 V/s after two CV cycles to −1 V (black), to −1.5 V (red), to −2 V (blue) and after regeneration of PTA by reimmersion in PTA solution (green).

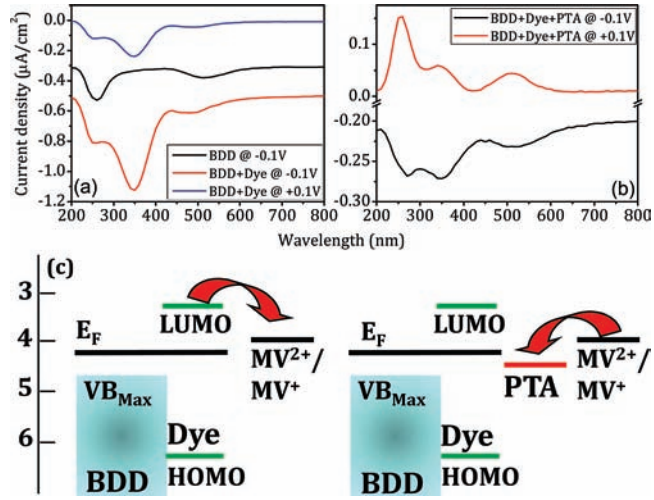

Figure 7. (a) Action spectrum of H-terminated BDD (black), molecular-dye-functionalized BDD (BDD + dye) at −0.1 V (vs Ag/AgCl) bias (red) and BDD + dye at +0.1 V bias (blue). (b) Action spectrum of electrostatically self-assembled PTA on molecular-dye-functionalized BDD (BDD + dye + PTA) at −0.1 V bias (black) and at +0.1 V bias (red). (c) Schematic drawing of energy level alignments (with respect to vacuum level) between BDD/dye/MV^{2+} and BDD/dye/PTA/MV^{2+} and their preferred electron flow direction.

can be cathodically stripped off (> −1 V) and regenerated by reimmersing in PTA solution (Figure 6). Such controllable release of electrostatically self-assembled PTA may be useful for electronics or sensing applications.

Photoelectrochemical Characterization. Photoelectrochemical measurements were performed in 0.1 M Na_2SO_4 solution containing 5 mM methyl viologen (MV^{2+}) as electron carrier under variable wavelength monochromatic irradiation. From Figure 7a, the action spectrum of H-terminated BDD shows a photocurrent peak at around 250 nm which is attributed to the absorbance characteristic of methyl viologen.[30] A small board peak at 520 nm is possibly due to defect-related absorption inherent with CVD diamond.[31] After grafting of the molecular dye, it led to the appearance of a photocurrent peak at 350 nm attributed to the molecular dye absorption at the diamond−molecular dye−solution interfaces. The VAMP-simulated absorption maximum of the molecular dye is calculated to be 340 nm (Figure 8), which agrees very well with the absorption peak at

(27) Stotter, J; Show, Y.; Wang, S.; Swain, Greg *Chem. Mater.* **2005**, *17*, 4880.
(28) Bard, A. J.; Faulkner, L. R. *Electrochemical Methods: Fundamentals and Applications*; John Wiley & Sons: New York, 2000.
(29) Jiang, K.; Zhang, H.; Shannon, C.; Zhan, W. *Langmuir* **2008**, *24*, 3584.
(30) Zak, J. K.; Bulter, J. E.; Swain, G. M. *Anal. Chem.* **2001**, *73*, 908.
(31) Nesládek, M.; Meykens, K.; Stals, L. *Phys. Rev. B* **1996**, *54*, 5552.

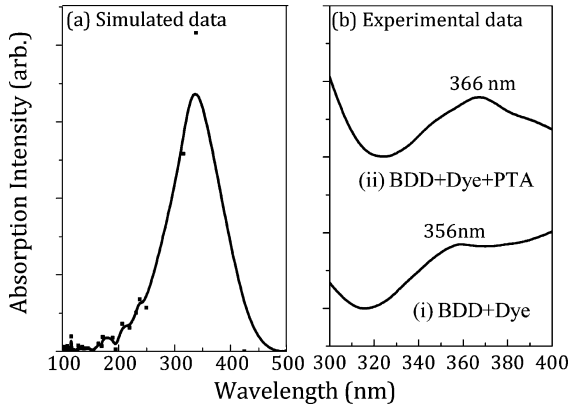

Figure 8. (a) UV−visible spectrum of molecular dye simulated using VAMP. (b) Solid-state UV−visible spectrum of (i) molecular-dye-functionalized BDD (BDD + dye) and (ii) after electrostatic self-assembled of PTA (BDD + dye + PTA).

353 nm in the UV−visible spectrum of molecular dye grafted on diamond (BDD + dye). It can be seen that the photocurrent peak at 350 nm for BDD + dye (Figure 7a) mirrors the absorption peak in the UV−visible spectrum at 353 nm (Figure 8b). After electrostatic binding to PTA, the absorption peak of the composite film is slightly broadened and red-shifted to 366 nm with similar absorption intensity. However, the action spectrum of BDD + dye + PTA at the same applied bias (−0.1 V vs Ag/AgCl) shows a significantly reduced photocurrent density compared to BDD + dye despite their similar absorption intensity. This implies that the addition of PTA impedes the preferred electron flow.

Before the addition of PTA, the preferred electron flow direction is from LUMO of the dye to the electron carrier, MV^{2+}, and this is favored by the application of a negative bias. The application of a small positive bias (+0.1 V) caused a reduction in the photocurrent obtained throughout the spectrum, as the positive bias retarded the preferred electron flow direction from LUMO of dye to the electron carrier, MV^{2+}. We found that the electrostatically bound PTA molecules could modulate the direction of current flow from the diamond to MV^{2+}. In the absence of the PTA molecules, at +0.1 V electrode bias (Figure 7a), the current is negative. In the presence of surface-bound PTA molecules, at the same applied voltage of +0.1 V (Figure 7b), the current becomes positive. The reversal of current can be explained by the chemical potential of PTA which lies below that of MV^{2+}, thus favoring electron flow from the latter to the former, as shown in the energy level alignment diagram in Figure 7c. Following the photoexcitation of the dye, a hole is created in the HOMO. In this case, electron is transferred from the MV^{+} to PTA, and from PTA to the HOMO of the dye. The energy levels of the BDD and grafted molecular dye, with respect to vacuum level, were determined using ultraviolet photoelectron spectroscopy (see Supporting Information). The chemical potential of MV^{2+}/MV^{+} is taken to be 4.0 eV below vacuum level.[32] The first redox potential of PTA at around −0.1 V (vs Ag/AgCl) is used to determine its chemical potential below vacuum level (4.3 eV).

The electrostatic assembly of PTA on the dye-diamond surface broadens the photocurrent conversion spectra window to 500 nm and beyond. It is well-known that the UV irradiation of PTA film can result in the appearance of absorption bands in the visible and near-IR regions arising from photoinduced reduction of W^{6+} into W^{5+}, giving rise to intervalence charge transfer bands between adjacent W^{5+} and W^{6+} sites.[33] PTA, being a photochromic molecule,[34] can trap photogenerated electrons accompanied by the conversion of W^{6+} into W^{5+} ions, the photochromic response being drastically enhanced in the presence of photohole scavengers like methyl viologen.[35] The presence of these convertible W^{6+} and W^{5+} redox species can give rise to both cathodic and anodic currents.[32] The simultaneous injection of electrons and holes into the interstitial sites in PTA can be driven photoelectrochemcially, thus in this case at both negative and positive bias, we can observe current flow with quite similar magnitudes in Figure 7b. The ability to have current reversal at the same applied voltage by a reversible tethering of molecular species on the electrode surface may be useful for controlling the physical properties of electrochemical deposited metallic nanostructures. Building photochromic materials like PTA on an optically transparent and conducting diamond platform opens up the possibility of combining photochromic coloration with electrochemical erasing.

IV. Conclusion

We have demonstrated a method to build a hierachical assembly of organic−inorganic hybrid films on diamond. The versatility of this method is that different inorganic systems can be assembled on the organic wire platform by electrostatic assembly. In particular, an inorganic system based on polyoxometalate provides functional components for constructing modular molecular nanosystems which can mediate charge transfer between diamond and electrolyte. The chemical stability and optical transparency of the diamond platform allows optical and electrical actuation of such nanosystems in corrosive media, as demonstrated by the reversible tethering of PTA *via* cathodic stripping and electrostatic assembly.

Acknowledgment. K. P. Loh acknowledges ARF-MOE Grant "Structure and Dynamics of Molecular Self-Assembled Layers. R-143-000-344-112."

Supporting Information Available: UPS data for determination of energy levels. This material is available free of charge via the Internet at http://pubs.acs.org.

JA908131T

(32) Shin, D.; Watanabe, H.; Nebel, C. E. *J. Am. Chem. Soc.* **2005**, *127*, 11236.
(33) Papaconstantinou, E. *Chem. Soc. Rev.* **1989**, *18*, 1.
(34) Yamase, T. *Chem. Rev.* **1998**, *98*, 307.
(35) Bahnemann, D. W.; Hilgendorff, M.; Memming, R. *J. Phys. Chem. B* **1997**, *101*, 4265.